Synchronous high-voltage spindles in the cortex-basal ganglia network of awake and unrestrained rats

Cyril Dejean, ¹ Christian E. Gross, ^{1,2} Bernard Bioulac ^{1,2} and Thomas Boraud ¹

¹Laboratoire de Neurophysiologie, CNRS UMR 5543, Université Victor Segalen Bordeaux 2, 146 rue Leo Saignat, 33076 Bordeaux cedex, France

²Laboratoire Franco-Israélien de Neurophysiologie et Neurophysique des Systèmes, Bordeaux Centre Hospitalier Universitaire, 33076 Bordeaux cedex, France

Keywords: electrophysiology, HVS, oscillations, striatum, substantia nigra

Abstract

Synchronous oscillations in various frequency ranges have been recorded in several nuclei of the basal ganglia (BG) and are thought to be an information processing mechanism. High-voltage spindles (HVSs) are 5–13 Hz spike-and-wave oscillations, which are commonly recorded in rats and which have been reported in some recent studies where their occurrence in the BG has been investigated. We recorded single neurons and local field potentials (LFPs) simultaneously in the motor cortex, striatum and substantia nigra pars reticulata (SNr) of the freely moving rat. We took advantage of the high level of synchronization observed during HVSs to study signal transmission in the cortex–BG network in the awake animals. The results show that LFPs are synchronized in the motor cortex, striatum and SNr during HVS episodes and that the latter propagate from the cortex to the SNr via the striatum. Moreover, >50% of single neurons in each of these structures are triggered by the HVS. Following the discharge of cortical cells, SNr neurons are first inhibited after \sim 19 ms and then activated after \sim 45 ms. This response is probably driven by the direct and indirect pathways, respectively, without any involvement of the hyperdirect pathway. Here, it is shown that cortex–BG connectivity can be studied using physiological signals in the freely moving animal as opposed to artificial stimulation under anaesthetized conditions. This opens the door to further studies under various experimental conditions, such as animal models of basal ganglia disorders.

Introduction

The basal ganglia (BG) are a complex interconnected network which process cortical information and are thus involved in higher brain functions such as motor control (Graybiel *et al.*, 1994; Graybiel, 1995). Synchronous oscillations have recently been shown to be a possible mechanism for information processing in the BG (Hutchison *et al.*, 2004) and have been recorded in several BG nuclei of parkinsonian patients (Brown, 2003) and animal models of Parkinson's disease (Bergman *et al.*, 1994; Goldberg *et al.*, 2004; Sharott *et al.*, 2005). However, the transmission of rhythmic activities is still poorly understood (Boraud *et al.*, 2005).

In the BG of healthy rats, oscillations can be observed in various frequency ranges including, for example, the 30–60 Hz gamma rhythms (Brown *et al.*, 2002; Masimore *et al.*, 2005), slow-wave activity in anaesthetized animals (Goldberg *et al.*, 2003) or high-voltage spindles (HVSs). The latter remain the most prominent oscillations in awake rats. They range from 5 to 13 Hz and have a characteristic spike-and-wave shape. They have been studied mainly in somatosensory systems (Robinson *et al.*, 1978; Nicolelis *et al.*, 1995; Kandel & Buzsáki, 1997) and only a few recent studies have seriously investigated their occurrence in the BG (Deransart *et al.*, 2003; Berke *et al.*, 2004; Slaght *et al.*, 2004; Magill *et al.*, 2005; Paz *et al.*, 2005).

Correspondence: Dr Thomas Boraud, as above. E-mail: thomas.boraud@umr5543.u-bordeaux2.fr

Received 1 August 2006, revised 26 October 2006, accepted 16 November 2006

The mechanism by which the HVSs propagate to the substantia nigra pars reticulata (SNr) is still poorly understood. An understanding of this mechanism could help to elucidate the pathophysiology of Parkinson's disease. Striatum and SNr are the principal input and output structures of the BG in rodents (Parent & Hazrati, 1995). They are functionally connected in a top-down fashion, forming the direct pathway of the BG. The SNr also receives information from striatum via the globus pallidus (GP) and subthalamic nucleus (STN), through the so-called indirect pathway (Smith et al., 1998). A third pathway, referred to as 'hyperdirect', links the cortex and SNr via the STN (Nambu et al., 2002). So far, studies of single-neuron functional connectivity and BG pathways have focused mainly on anaesthetized rats, using cortical microstimulation (Maurice et al., 1999; Kolomiets et al., 2003; Magill et al., 2004; Mallet et al., 2005). However, this approach is problematic as electrical stimulation of the cortex silences cortical neurons for 200 ms, and because anaesthetics are known to alter neuronal firing behaviour (Windels & Kiyatkin, 2006). Recent studies in the freely moving rat showed that cortical HVSs drive neurons in the striatum of normal animals (Berke et al., 2004) and in the SNr of epileptic rats (Deransart et al., 2003) of the genetically absence epilepsy rat from Strasbourg (GAERS) strain. However, no such single neurons were recorded simultaneously from more than one structure.

The goal of the present study is to investigate HVS transmission, in order to unravel the mechanisms of signal processing through the cortex–BG funnel in physiological conditions. For this purpose, local field potentials (LFPs) and multiple single units were recorded

simultaneously in the motor cortex, striatum and SNr of freely moving animals, without any artificial stimulation.

Materials and methods

Animals

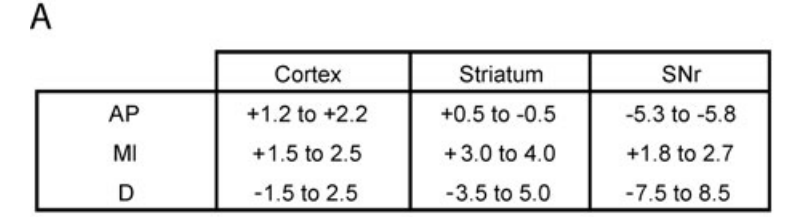
Six male Wistar rats (350–400 g; Depré, Saint Doulchard, France) were maintained under standard housing conditions at constant temperature $(22 \pm 1 \, ^{\circ}\text{C})$, humidity (relative, 30%), and 12-h light–dark cycles (light period 08.00-20.00 h). Water was available ad libitum. Food intake was limited to 10–20 g per day to maintain constant animal weight. Animal care and surgery were consistent with the National Institutes of Health Guide for the Care and Use of Laboratory Animals and European Community Council directive of November 24, 1986 (86/609/EEC) Comité Ethique de lu Région Aquitaine.

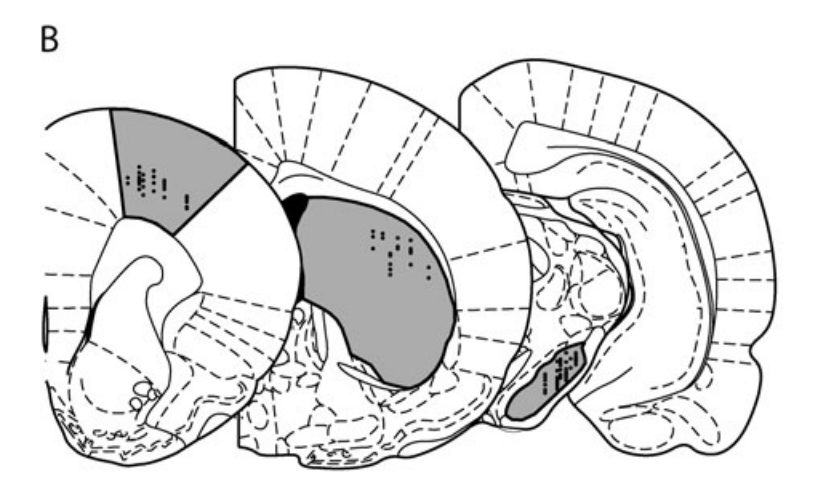
Head-stage

A home-made head-stage was designed for the purpose of this experiment. Electrodes were nickel-chrome formvar-insulated wires (diameter 15 µm; A-M System, Carlsborg, WA, USA) whose impedance was adjusted to between 0.5 and 2 M Ω . The head-stage consisted of bundles of four to six electrodes inserted in 29-gauge stainless steel cannulae (Phymep, Paris, France) mounted on three independent microdrives for a total of 16 microelectrodes. The cannulae were wired together and used as a reference electrode. The head-stage also provided a syringe guide designed for inducing chemical lesions needed in other experiments. The 3-D coordinates of the bregma and the bundles (see Fig. 1) were predefined on the headstage using a stereotaxic frame (Kopf, Tujunga, CA, USA) and an atlas of the rat brain (Paxinos & Watson, 1998). Several studies show that corticostriatal and striatonigral projections are somatotopically organised in the rat (Deniau et al., 1996; Kolomiets et al., 2003; Mailly et al., 2003). The results from these studies were used to define the coordinates of the electrodes and it can therefore be assumed that recordings reported here were made within interconnected regions. During surgery, the predefined bregma on the head-stage was adjusted to the actual bregma coordinates on the animal's skull so that the electrode bundles were situated just above their recording sites. The complete head-stage was then moved down so that the electrode tips were below the brain surface; coordinates were according to Paxinos & Watson (1998).

Surgery

The rats were operated on under xylazine (60 mg/kg i.p.; Rompun, Bayer, Germany) and ketamine (100 mg/kg i.p.; Virbac, Carros, France) anaesthesia. Recording targets were located with a stereotaxic frame (Kopf); above these, holes were drilled in the skull. The headstage was lowered and the holes filled with vaseline (Vaseline; Gifrer Barbezat, Decines, France). The head-stage was then attached to the animal's skull with glue (Superbond; Sun Medical Co., Japan), dental cement (DentalonPlus; Heraeus Kulzer, Hanau, Germany) and stainless steel screws. Before the end of anaesthesia, electrophysiological activities were recorded in order to make fine adjustments of the electrode positions when recorded signals did not agree with the characteristics of the targeted structures. The animals were given ketoprofen (Ketofen 2 mg/kg, s.c.; Merial, Lyon, France) following surgery, and again 24 h later, for pain relief. The animals were then allowed to recover for 10 days before the first recording session.





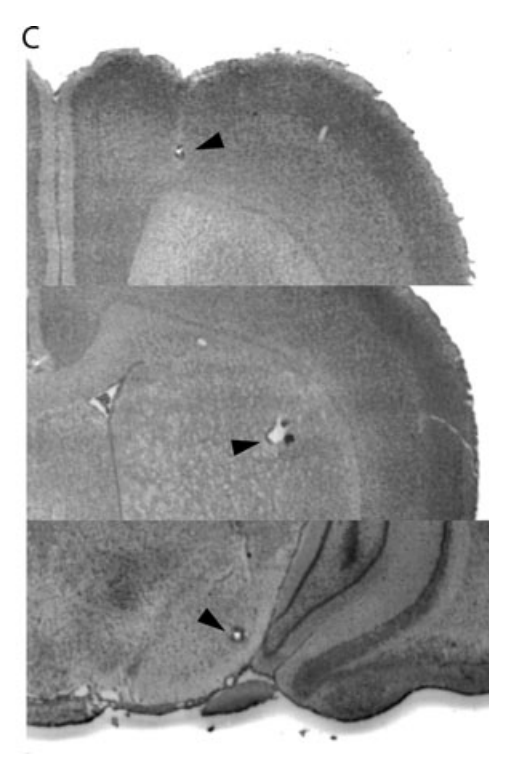


FIG. 1. (A) Coordinates of the electrode tips. The values are distances from bregma (mm). AP, anteroposterior coordinates; ML, mediolateral coordinates; D, depth according to brain surface. (B) Schematic localization of the recording sites inside the motor cortex (left), striatum (centre) and SNr (right). Dots show the locations of recorded neurons in each of the six rats. (C) Coronal sections stained with Cresyl Violet at the recording sites in the motor cortex (top), striatum (centre) and SNr (bottom). Arrows show electrolytic microlesion locations. All slices have been taken from the same rat.

Data acquisition

Daily recordings ran for 1 h in a circular arena (40 cm diameter), during which physiological and behavioural activities were simultaneously recorded. Neural signals were preamplified ×25 (MiniHeadStage; AlphaOmega Engineering, Nazareth Illit, Israel), then amplified by a multichannel processor and digitized at a rate of 50 kHz (MCP; AlphaOmega Engineering). The raw signal was stored for further analysis at the lower rate of 12.5 kHz (AlphaMAP; AlphaOmega Engineering). In parallel, it was also filtered (300 Hz-3 kHz) for online spike discrimination using a template-matching procedure (Multi Spike Discriminator; AlphaOmega Engineering). Discriminated spikes were stored synchronously with the raw signal. The movements of the animals were recorded simultaneously with a video tracking system (VTS; Plexon Inc., TX, USA). Their positions and the video recording were sampled at 30 Hz and stored separately from the neural data using videocapture software (Cineplex; Plexon Inc.). Neural and behavioural signal recordings were triggered simultaneously and the exact timing of each position and video frame was also sent to the AlphaMAP and stored within the neural data files for off-line synchronization.

Histology

Following the final recording, the rats were given a lethal dose of pentobarbital (Penthobarbital Sodique; CEVA, Libourne, France). Immediately after the injection, electrical microlesions (30 $\mu A, 10$ s) were induced by passing an anodal current through one electrode at each recording site. The brain was then quickly removed and frozen in an isopentane bath at $-80~^{\circ}\text{C}$ for histological analysis. Coronal brain sections (20 μm) were cut and those encompassing the motor cortex, striatum and SNr were mounted on slides for electrode placement verifications. These slices were stained with Cresyl Violet for structural identification. The recording tracks and sites were then established by observing the marks left by the cannulae and the electrolesions.

Data analysis

Signal processing

The striatum contains several types of neuron, among which the medium spiny neurons (MSNs) are the only output neurons. In this study, only MSNs discriminated according to shape and frequency criteria are described. Cells with a mean hyperpolarization duration $> 300~\mu s$ and a firing rate <2 spikes/s were classified as MSNs (Berke et al., 2004). Cells with a mean hyperpolarization duration $<300~\mu s$ and a firing rate >1 spike/s were classified as interneuron-like neurons. Cells not satisfying one of these two conditions were rejected. Very few interneurons (n = 3) were recorded during this study. As a consequence, results related to them are not presented here. All striatal neurons with waveform valleys $<300~\mu s$ and mean discharge rates <1 spike/s (Fig. 2) were rejected.

The cortex contains pyramidal neurons and interneurons. Both types were discriminated using a time criterion (Bartho *et al.*, 2004). Cells presenting a peak–valley duration > 500 μ s were classified as putative pyramidal neurons (n=31; Fig. 2). Other cells were classified as interneurons (n=2). Only pyramidal projecting neurons were considered in this study. Corticostriatal neurons only represent a subset of projection neurons. The setup and recording procedure described here does not allow connectivity tests, such as antidromic stimulation or marker tracing, to be performed in order to detect whether neurons were actually sending axons to the striatum. It was assumed that a proportion of the recorded cortical neurons were putative corticostriatal neurons. Moreover, simultaneous multiple

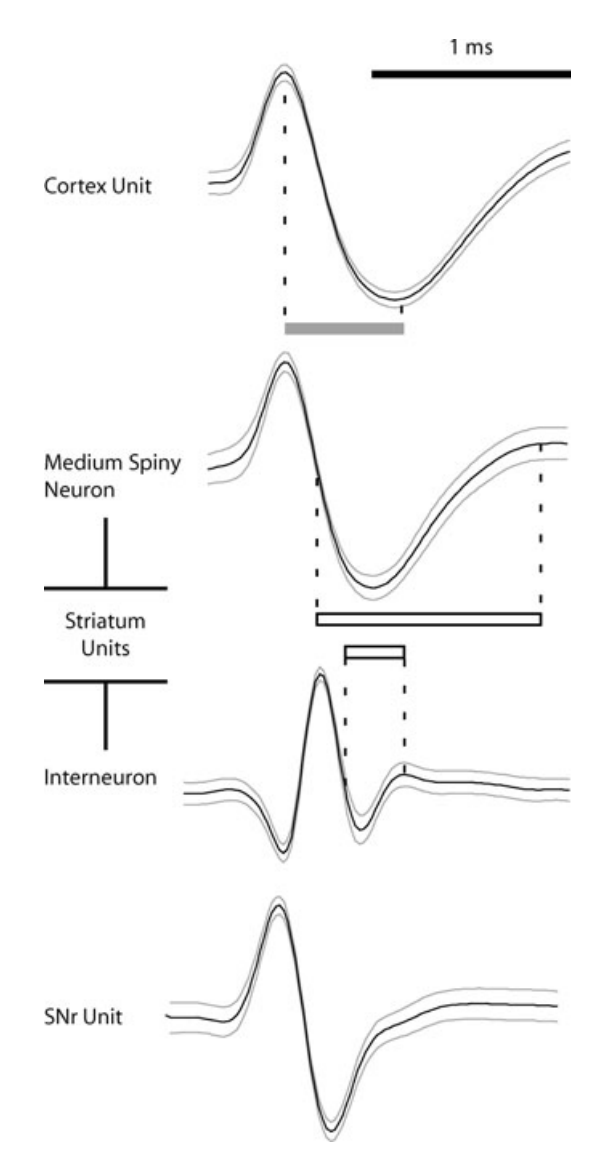


FIG. 2. Typical waveforms recorded in motor cortex, striatum and SNr. The waveforms of four simultaneously recorded cells. Solid lines, mean spike shape; shaded lines, SD. The shaded bar shows the peak–valley duration. The open bar shows the duration of the negative deviation. Bin width, 20 μs. Discrimination was performed online (see Materials and methods). From top to bottom: motor cortex neuron (771 spikes, mean firing rate 2.89 spikes/s, peak–valley duration 0.59 ms, hyperpolarization duration 1.11 ms); striatal MSN (102 spikes, 0.201 spikes/s, 1.13 ms), striatal interneuron (5041 spikes, 3.42 spikes/s, 0.29 ms) and SNr neuron (18 181 spikes, 41.6 spikes/s, 0.77 ms).

single-unit recordings showed that projecting neurons (thus including corticostriatal) fire synchronously in a short time window during HVSs (Kandel & Buzsáki, 1997). Therefore, in our recordings the overall firing time of cortical neurons is probably representative of the corticostriatal population itself.

HVS discrimination

HVSs exhibit two main features, namely a spike-and-wave pattern and an oscillation frequency ranging between 5 and 13 Hz. Both criteria were used to detect the beginning and end of these episodes. For frequency criteria, a threshold on the instantaneous power spectral density (PSD) of LFPs was used. LFPs were first filtered (1–200 Hz), using a second-order bandpass Butterworth filter, and then down-sampled (from 12500 Hz to 500 Hz). For each brain structure, the PSD

was computed every 100 ms using an overlapping sliding window with a length of 250 sample points (0.5 s). The instantaneous averaged PSD in the 5–13 Hz range was computed for each time step. Its value was deemed to have increased significantly when it passed the threshold (T) computed according to T = mean + 3 SD of the instantaneous PSD values over the whole recording session. Over-threshold time steps determined preliminary epochs. A pattern criterion was assessed manually. Preliminary epochs, within which the LFPs showed no typical spike-and-wave pattern, were rejected. Previous studies showed that HVS onset and end could occasionally differ between cortex and striatum (Berke et al., 2004). Because of the very large convergence from the cortex to the striatum, this lag can be attributed to the fact that onset and end may vary across cortical locations (Shaw, 2004). The HVS could have been transmitted to the striatum from a cortical location somewhat removed from that of the cortical recording electrode, thereby introducing an apparent onset delay. The same phenomenon could account for a delay in observed HVS endings. The analysis time frame was restricted to one ideal oscillation cycle, during which the cortex, striatum and SNr were all oscillating. To remove the lag-related bias, only those time intervals having overlapping preliminary epochs were taken into account, using Neuroexplorer software (Nex Technologies, Littleton, MA, USA).

HVS oscillation trough and peak markers were then discriminated within HVS epochs using temporal and voltage criteria with a C++ home-made routine running under Matlab (The Mathworks, Natick, MA, USA). Cortical electrodes were placed around the border of layers V and VI (~ 1.5 –2.5 mm below the surface) to record projection neurons. At this level, the earliest HVS spike component is negative (Kandel & Buzsáki, 1997). For this reason, cortical LFP markers were positioned at the troughs. As striatum and SNr spike components are positive, striatal and nigral markers were positioned at the peaks.

Behavioural analysis

Off-line discrimination of movement and rest episodes was carried out using Cineplex software (Plexon Inc., Littleton, MA, USA). Basal activity was characterized by the mean and SD speed (cm/s) during a typical rest episode for each rat. A threshold was then defined as the upper confidence limit (CL) = mean + 1.96 SD. The animal was considered to be active when its speed exceeded this threshold for >0.5 s. Movement time intervals were then correlated with electrophysiological data. The animal's activity level was quantified as the percentage of time spent by the animal moving during the recording.

Spectral characterisation of LFP

Power spectral densities of LFPs were computed by means of fast Fourier transform analysis, using sliding windows of 1250 samples (2.6) in the range 0-500 Hz (0.39 Hz resolution). Histograms were smoothed with a three-point Gaussian process.

Coherence was computed from the formula

$$Coherence_{ij} = (P_{ij} \times P_{ji})/(P_{ii} \times P_{jj})$$

where P is the average of the squares of the LFP spectra i and j. Former spectra were computed using the same method as described above (unless otherwise stated). Comparisons between coherence histograms computed during rest, movement and HVS episodes were made using a one-way ANOVA (with P = 0.05).

Characterisation of spike trains

Cross-correlograms show the conditional probability of a spike train at time t, on the condition that a reference spike occurs at time 0.

Considering the spike train to be a Poisson process, the crosscorrelogram CLs were computed using Neuroexplorer software (Nex Technologies) from the formula $CL = Z \pm 2.58\sqrt{Z}$, where Z = (spike)mean firing rate) × (crosscorrelogram bin size) / (number of reference spikes) with bin size = 2 ms and number of reference spikes >50. Auto-correlograms and cross-correlograms were considered positive if their value passed the CL criterion.

Power spectral densities of cross-correlograms were computed by fast Fourier transform analysis using sliding windows of 256 samples (1.25 s) in the range 0-200 Hz, yielding a resolution of 0.8 Hz. Histograms were smoothed with a three-point Gaussian process. The CL of power spectral density histograms were computed in the 3-50 Hz range as follows: CL = mean + 3 SD. Auto-correlograms and crosscorrelograms were considered oscillatory if any power spectral density value in the range 5–13 Hz passed the CL (with P < 0.01).

Oscillation frequencies of LFPs and neurons were compared by running a one-way ANOVA on frequency peak distributions of LFPs and auto-correlogram spectra during HVS epochs (with P=0.05). To test interindividual variations, the values of frequency peaks were compared in each rat using a two-way ANOVA (with P = 0.05). One factor was the rat number and the other factor was the type of data, i.e. the LFP or neuron auto-correlograms.

To ensure that the LFPs in each structure were oscillating in the same frequency range, the frequency peak values were compared in each structure using a Kruskal-Wallis one-way ANOVA on ranks (with P = 0.05).

Spike trigger averaging

Computations of spike trigger averaging (STA) give the mean voltage of an LFP at time t, on the condition that there is a reference spike at time 0. STA voltages were normalized using the maximum amplitude of HVS oscillations as follows:

normalized
$$STA_{ijk} = STA_{ijk}/(\max LFP_{jk} - \min LFP_{jk})$$

where i denotes the structure in which the reference neuron was recorded, i.e. the cortex, striatum or SNr, j denotes the structure in which the LFP was recorded, i.e. the cortex, striatum or SNr, and kdenotes the session during which LFP j was recorded. Only reference spikes which fired >50 spikes during HVS epochs were taken into account for this analysis. Normalized STAs were tested for significance of LFP-spike correlation using a CL computed as follows: $CL_{ijk} = mean_{ijk} \pm 3 SD_{ijk}$. STAs which crossed the confidence interval were defined as positive STAs (with P < 0.01). Positive STAs were then averaged in dimension k to assess STA_{ij} values.

In order to compare the influence of the spikes of each structure on normalized LFPs in one structure, an index was computed as follows: For cortex:

$$Index_{ij} = \sum_{l \to n}^{k} \frac{ValleyVoltage_{ijk}}{\underbrace{ValleyWidth_{ijk}}_{\theta_k}}$$

For striatum and SNr:

$$Index_{ij} = \sum_{l \to n}^{k} \frac{PeakVoltage_{ijk}}{\underbrace{PeakWidth_{ijk}}_{\theta_k}}$$

where i denotes the structure in which the reference neuron was recorded, i.e. the cortex, striatum or SNr, j denotes the structure in which the LFP was recorded, i.e. the cortex, striatum or SNr, and θk denotes the mean HVS period during session k in which LFP j and neuron i were recorded.

Time-lag distributions

Peri-event histograms were constructed with LFP markers in the cortex, striatum and SNr used as triggers (t_0) for the occurrence of spike trains and LFP marker trains at time t. For graphic representations, a 2 ms bin size and three-point Gaussian smoothing algorithm were used. Only triggers and spike trains which occurred > 50 times in HVS epochs were used for this analysis. Over a time frame of 100 ms before and after the reference event, peri-event peak and/or trough amplitudes were collected. Note that only SNr spike trains had significant troughs. The significance of peaks and troughs was tested using the same method as for cross-correlograms. The presence of a significant peak and/or trough defined a neuron as 'HVS-driven'. Peak times for spike trains and LFP marker trains were then used to construct time-lag averages around marker time points in each structure. Statistical comparisons of peak times were all carried out using a t-test (with P = 0.05).

The effect of the trigger on the lag between peaks and troughs was evaluated. For this purpose, the distributions computed by the above method were kept for each trigger and were first aligned with the cortical peak time. If the lag between cortical peak and striatal or nigral distributions does not depend on the trigger, the distributions associated with the latter, for each of the three markers, should be constant and therefore overlap. In this case, it may be considered that the temporal relationship between neuronal populations is stable and likely to reflect a strong functional link. The same analysis was performed with the distributions aligned with striatal peak times. Comparisons with aligned distributions were carried out using a t-test (with P=0.05).

Results

Lfp

HVSs were recorded in the LFP of the motor cortex, striatum and SNr in six rats (Fig. 3A and B). The frequency ranged between 5 and 13 Hz, with a respective mean and SD of 9.48 ± 2.06 Hz. No significant difference was found from one structure to another (one-way ANOVA on ranks, data not shown). The HVS duration $(1.106 \pm 0.86 \text{ s})$ as well as the percentage of time spent in this brain state $(5.83 \pm 7.2\%)$ within a recording session varied widely across rats and recording sessions. Behavioural analysis during HVS episodes revealed that the rats were awake and resting quietly whilst remaining responsive to tactile, auditory and visual stimuli. Moreover, no whisker twitching movements were observed during HVSs.

The coherence of each LFP combination, i.e. cortex-striatum, striatum–SNr and cortex-SNr, was significantly higher during HVSs, over the frequency range between 5 and 13 Hz, than during rest or movement episodes (Fig. 4).

Single neurons

Thirty-one neurons were recorded in the motor cortex, 20 MSNs in the striatum and 36 neurons in the SNr. Discharge rates during HVSs were 2.13 ± 2.11 spikes/s in the cortex, 0.78 ± 0.63 spikes/s in the striatum and 16.9 ± 8.11 spikes/s in the SNr. No significant changes were observed between HVS episodes and other epochs.

During HVSs, a large number of neurons showed significant oscillatory auto-correlograms (average of 46%) and cross-correlograms (average of 37%) in the 5-13 Hz band (Fig. 5, Table 1). These

percentages of oscillatory auto- and cross-correlograms were significantly higher during HVSs than during rest or movement episodes (Fig. 5C; one-way ANOVA on ranks, with P < 0.05).

Cortex and SNr units displayed a reproducible discharge pattern during HVSs, firing in > 50% of oscillation cycles, while striatal units had a very sparse firing mode (Fig. 3B). As a consequence, few showed significant oscillatory auto-correlograms (20% of striatal population) compared to cortical (55%) and nigral (53%) neurons. However, the presence of significant oscillatory cross-correlograms revealed the rhythmic nature of their relationship with cortex and SNr units (Table 1, Fig. 5A and B).

Interactions between LFP and single neurons

As shown above, LFPs and single neurons oscillated during HVSs. The distribution of peak frequency values of neurons and LFP showed no significant difference (two-way ANOVA, Rats × Neurons, Rats: F = 2.037, Neurons: F = 0.087 and Rats × Neurons: F = 0.813).

When triggered by HVS markers, the majority of single units were found to be driven by LFP oscillations whenever the former were recorded (Table 2).

STA gives the averaged form of an LFP around the occurrence of a neuron's action potentials. STAs triggered by cortical neurons (Fig. 6A) had a smoother appearance as well as a larger amplitude than STAs triggered by striatal and SNr neurons (Fig. 6B and C). Raw LFPs in the SNr exhibited a positive and a negative component in each oscillation cycle (Fig. 3A and B). It is noteworthy that the mean STAs of cortical neurons did not present the negative deviation which can be seen on the raw signal (Fig. 6A). The STA index quantifies spike influence on LFPs (Fig. 6D–F). The STA index for cortical neurons was always significantly higher than that corresponding to SNr neurons. By comparing the indices for cortex and striatum neurons (Fig. 6D and E), it may be seen that the cortical influence on LFP was always larger, but that this difference was not significant for the LFP recorded in the SNr (Fig. 6F).

The precise time of neuron peak firing and LFP markers was investigated for cases where the former were triggered on cortical, striatal and SNr LFP markers (Fig. 7). Within the period of a single oscillation cycle, markers appeared first in the cortex, then in the striatum and finally in the SNr (Fig. 7A). On average, cortical LFP markers preceded those in the striatum by 10.4 ± 6.5 ms and those in SNr by 28.9 ± 9.3 ms. The striatum preceded SNr by 18.5 ± 10 ms. The distributions of the three markers were significantly different and therefore nonoverlapping (t-test, P < 0.05 for each pair). Single-neuron activities followed a similar temporal pattern when triggered by cortical markers (Fig. 7B top). Cortical peak firing (-5.8 ± 4.2 ms) preceded striatal peak (3.2 ± 3.9 ms), SNr trough (15.6 \pm 3.9 ms) and SNr peak (40.5 \pm 4.8 ms). The four distributions were significantly different and therefore nonoverlapping (t-test, P < 0.05 for each pair). This was again the case when spike trains were triggered by striatal LFP markers (Fig. 7B, middle). Cortex (-10.8 \pm 3.8 ms) preceded striatum (1.8 \pm 6.2 ms), SNr trough (9.6 \pm 4.4 ms) and SNr peak (48.5 \pm 5.4 ms). The distributions were significantly different (t-test, P < 0.05 for each pair). A noticeable change was observed when action potentials were triggered by SNr LFP markers (Fig. 8B, bottom), as the previous neuronal temporal layout had become disorganised. The MSNs $(-41.8 \pm 6.4 \text{ ms})$ now significantly preceded $(-22.5 \pm 6.3 \text{ ms})$, SNr troughs $(-18.9 \pm 3.2 \text{ ms})$ and SNr peaks $(21.1 \pm 3.5 \text{ ms})$. No difference was found between the cortex and SNr troughs (t-test, P = 0.585) although both significantly preceded the SNr peak (*t*-test, P < 0.05 for both).

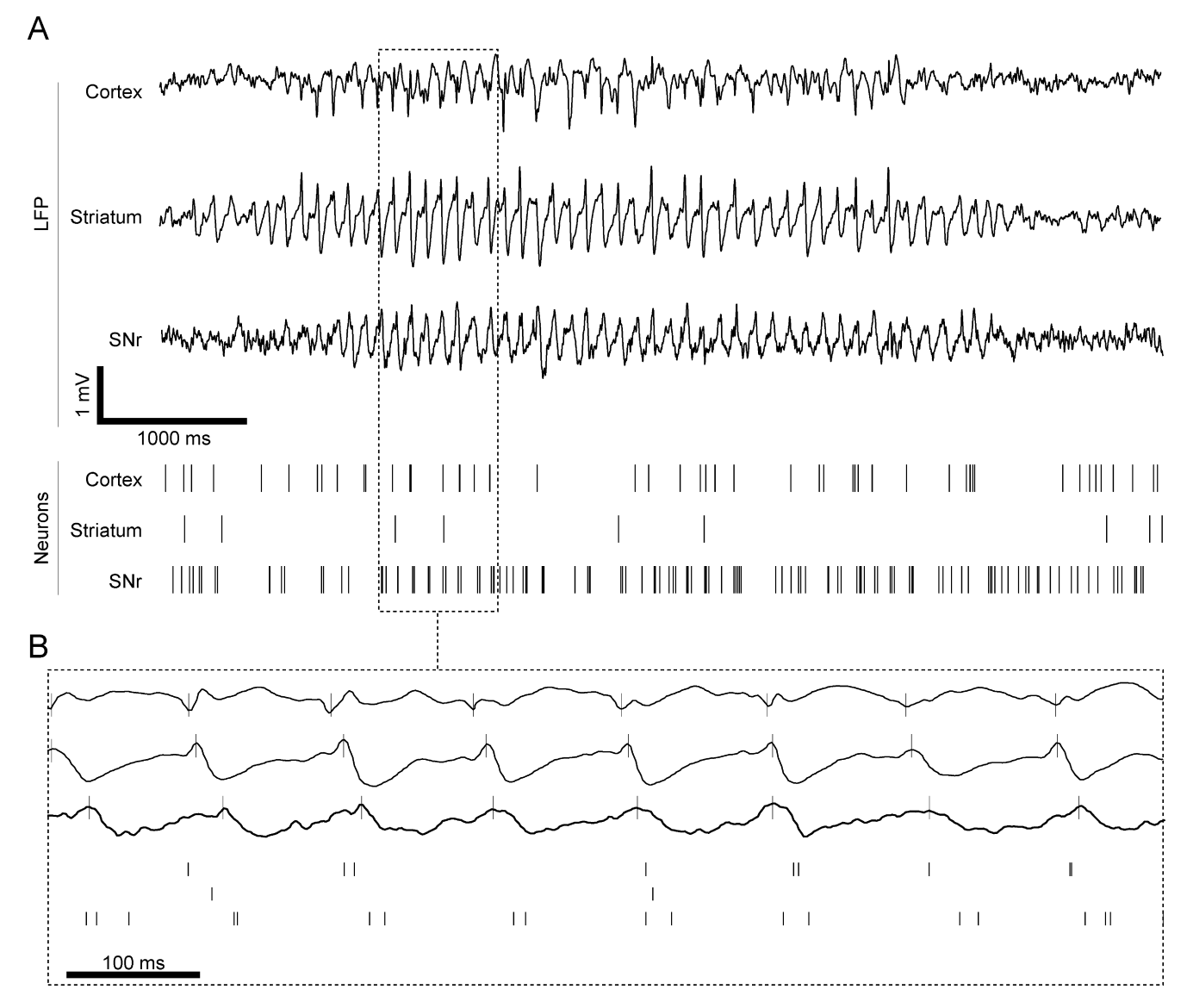


FIG. 3. LFPs and synchrony with single units during high-voltage spindles. (A) Example of LFPs and a single unit's activity during a typical HVS simultaneously recorded in the motor cortex, striatum and SNr. (B) In the dashed frame, a closer view shows three neurons which underwent rhythmic entrainment during the spindle. The positions of the local maxima and minima during the HVS episodes are indicated by markers plotted on the LFP traces. The cortical trough, striatal and SNr peaks are labelled (see Materials and methods). Motor cortex neurons fired one or two spikes for $\sim 50\%$ of oscillation cycles. Striatal neurons presented a sparse discharge mode. Occasionally, they fired only a single spike per cycle. SNr neurons fired several spikes during almost every oscillation cycle.

The effect of trigger type on the lag between peak and trough time distributions was tested. When aligned with the cortical peak (Fig. 7C, top), the lags relative to LFP markers and to SNr peak distributions showed no difference, no matter which trigger was used (t-test, P = 0.146 and P = 0.328, respectively). In contrast, the lags relative to the striatal peak and SNr trough distributions varied significantly as a function of trigger (t-test, P < 0.05 for both). Similarly, when aligned on the striatal peak (Fig. 7C bottom), the lags relative to the SNr trough distributions showed no difference, no matter which trigger was used (t-test, P = 0.382). In contrast, the lags relative to the cortical peak, SNr peak and LFP marker distributions varied significantly as a function of the trigger (t-test, P < 0.05 for each).

To summarise, two different putative functional couplings emerged. On the one hand, the cortex, SNr peak and LFP markers were clearly locked to each other as their relative distributions were not trigger-sensitive. One the other hand, striatal peaks and SNr troughs remained locked to each other although their lags relative to other distributions were trigger-sensitive.

Discussion

The present results show that commonly recorded HVS episodes are consistent in the motor cortex, striatum and SNr of freely moving rats (Figs 3 and 4). To the best of the authors' knowledge, this is the first evidence of the presence of neurons driven by cortical HVSs in normal rat strains. These data suggest that SNr neurons are driven first by inhibitory input from the direct pathway and then by the excitatory input from the indirect pathway. Consistent with previous studies in both normal and GAERS rats, synchronous HVSs were found in neurons of the input (striatum) and output (SNr) BG nuclei, and it is therefore likely that synchronous HVSs spread to the entire BG network.

Origin of LFPs in BG during HVSs

Despite the strong oscillations present in striatal LFPs, HVSs are not associated with prominent synchronized activity of striatal projection

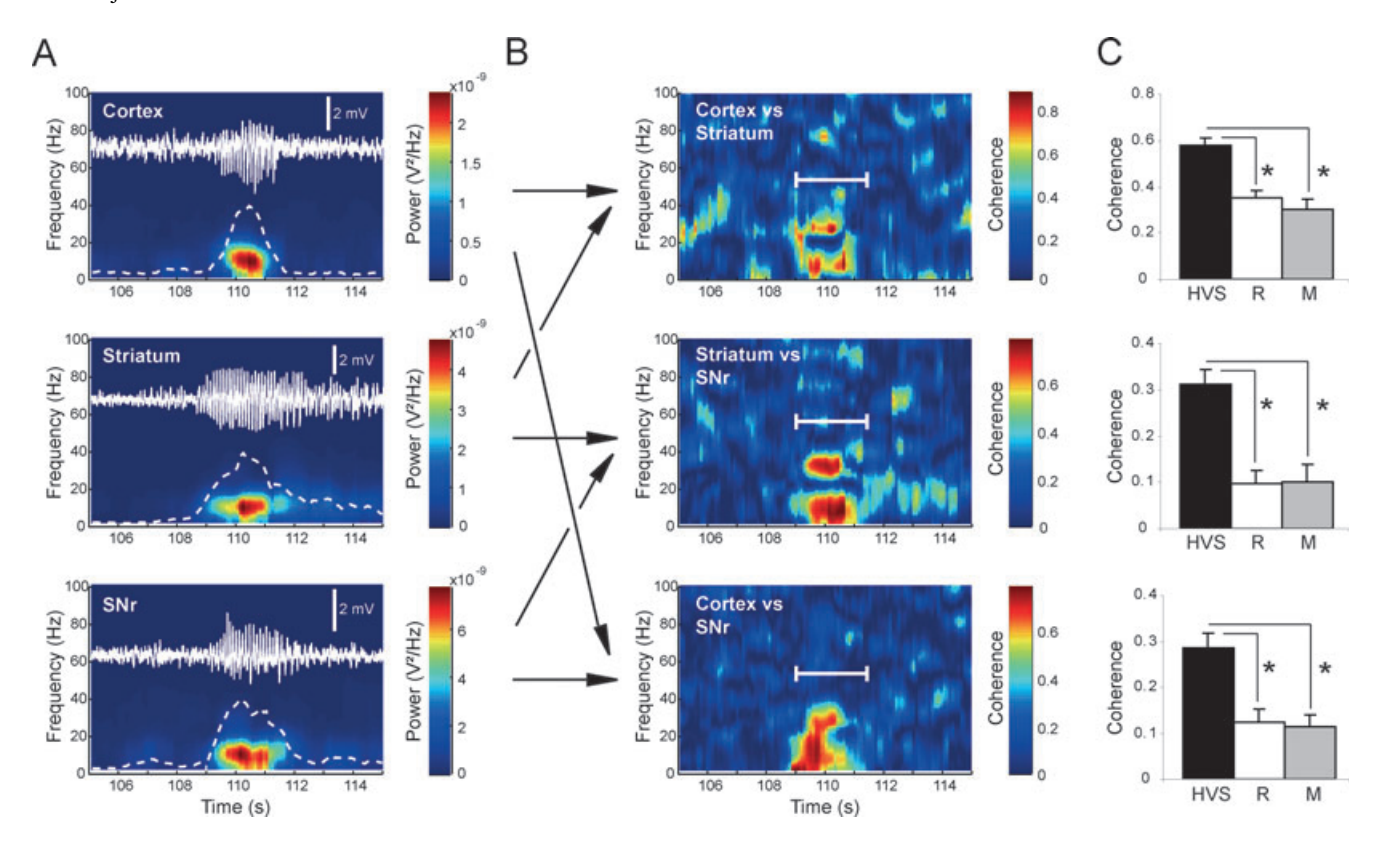


FIG. 4. Spectral analysis of LFPs during high-voltage spindles. (A) Example of simultaneously recorded LFPs in the cortex (top), striatum (middle) and SNr (bottom), together with their power spectral density (0-100 Hz) as a function of time. Display windows are centred on the onset of a typical episode of HVS. The superimposed solid line shows the raw LFP trace and the broken line represents the value of the LFP mean power spectrum in the 5-13 Hz range. This value is used to delineate HVS episodes (see Materials and methods). The power value is plotted in pseudo colours (scale on the right). The LFP sampling rate was 500 Hz and the power spectral density was computed every 100 ms with a 250-point overlapping sliding window (0.5 s). (B) Coherence as a function of time between each pair of LFPs shown in A: from top to bottom, cortex and striatum, striatum and SNr and cortex and SNr. The coherence value is plotted in pseudo colours (scale on the right). Arrows indicate the structures which are considered for coherence computations. The white interval labels the HVS epoch detected with the use of mean power spectra in the 5-13 Hz range (shown in A). (C) Population average (n=6) of coherence in the 5-13 Hz range, between cortex and striatum (top), striatum and SNr (middle), and cortex and SNr (bottom). Coherence values were compared during HVS (black), rest without HVS (R, white) and movement episodes (M, grey). *P < 0.05 between coherence values (one-way ANOVA).

neurons, as previously shown (Berke et al., 2004; Slaght et al., 2004). However, it has already been shown that LFP oscillations are mainly the consequence of striatal afferents. Indeed, it has been previously reported that rhythmic cortical activity drives a synchronized oscillation of the membrane potential of MSNs (Tseng et al., 2001; Slaght et al., 2004). Striatal HVSs may thus reflect cortical afferent activity as well as MSN membrane potential oscillations.

LFPs in the SNr are more probably due to the strong rhythmic activity observed in most neurons. However, the SNr is a small structure and the recorded field could therefore be influenced by neighbouring structures. In particular the STN, which is very close to the SNr, exhibits strong oscillations in its LFP during HVSs. Due to the monopolar approach used here, the level of focality of the recorded LFPs cannot be assessed. There is, however, evidence that the SNr LFP is not, or is only very weakly, influenced by volume conduction of STN LFP: STN peaks recorded in a previous study (Magill *et al.*, 2005) follow the cortical trough by 2.7 ms, whereas it is shown here that the SNr follows the cortex by 28.9 ms. In view of this discrepancy in LFP peak times and the fact that SNr and STN are almost contiguous in the rat brain, it is very unlikely that the STN volume-conducted LFP significantly influenced the LFP of the SNr in the present recordings.

Synchronous HVSs in the input and output nuclei of the BG

HVSs were recorded synchronously in the LFP of the input and output of the BG. It is thus likely that HVSs spread to the entire BG network of normal rats. This conclusion is strongly supported by previous studies, in both normal and GAERS rats, which reported the same synchronized HVSs in STN and the cortex of freely moving rats (Vergnes *et al.*, 1990; Magill *et al.*, 2005) as well as in the STN and GP of anaesthetized rats (Paz *et al.*, 2005).

It is shown here that the majority of neurons in the motor cortex, striatum and SNr are simultaneously driven by LFP markers during HVS episodes (Table 1). Moreover, a substantial percentage of cross-correlations of simultaneously recorded single units show a dynamic link between neurons, and therefore suggest that these are functionally linked and that, during HVSs, this relationship is transiently expressed in an oscillatory fashion. This confirms what has been suggested by previous recordings in individual structures (Deransart *et al.*, 2003; Berke *et al.*, 2004; Slaght *et al.*, 2004; Magill *et al.*, 2005; Paz *et al.*, 2005). Moreover, the presence of rhythmically driven neurons in each structure, and of time lags between structures, excludes the hypothesis that the LFPs reported here were simply volume-conducted through the brain.

The influence of cortical neurons on the activity of the network is critical (Fig. 6). Among all neuronal categories recorded during this

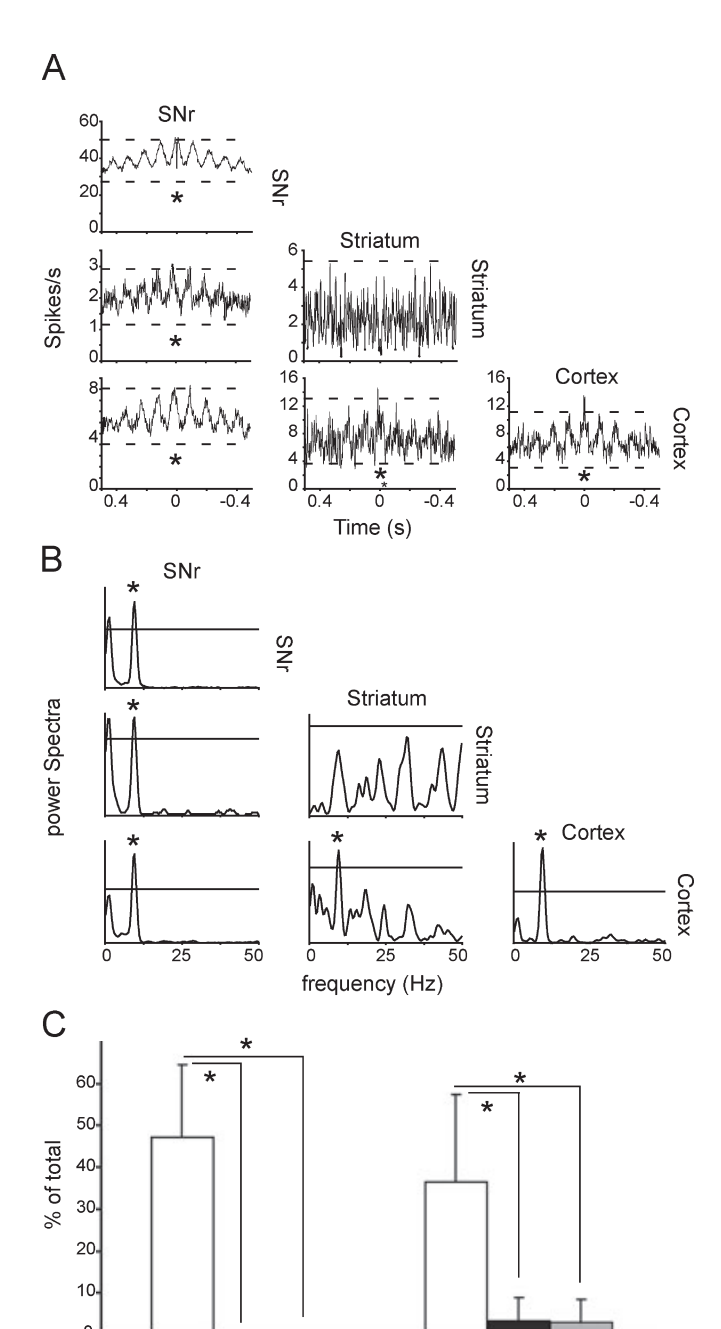


Fig. 5. Neurons exhibited oscillatory firing during HVSs. (A) Cross-correlogram matrix for three neurons simultaneously recorded in the motor cortex, striatum and SNr. Dashed lines represent the confidence interval of the mean (P = 0.05; see Materials and methods). An asterisk (*) indicates a significant peak. (B) Power spectral densities of the cross-correlograms shown in A. The line represents the significance threshold of the power peak (P = 0.01); see Materials and methods). An asterisk (*) indicates a significant peak. (C) Ratio of oscillatory auto- (AC, left) and cross-correlograms (CC, right) in the 5-13Hz range during HVSs (black bars), rest without HVS (R, white bars) and movement episodes (M, grey bars). The percentage of oscillating auto- and cross-correlograms was significantly higher during HVS epochs than during rest or movement episodes. *P < 0.05 (one-way ANOVA).

HVS

R

Oscillatory CC

M

HVS

R

Oscillatory AC

М

study, cortical neurons exhibited more stable and sharp firing than striatal and SNr neurons. It is thus likely that the former are responsible for striatal and SNr driving. Nevertheless, as expected,

TABLE 1. Ratio of oscillatory auto-correlograms (in bold) and cross-correlograms during HVSs

	Cortex		Striatum		SNr	
	$(n/\text{total}^{\ddagger})$	(%)	(n/total)	(%)	(n/total)	(%)
Cortex Striatum SNr	17/3* 24/54 [†] 30/84 [†]	55* 44 [†] 36 [†]	4/20* 21/64 [†]	20* 33 [†]	19/36*	53*

^{*}Auto-correlograms; †cross-correlograms; n, number of oscillatory correlograms; ‡total number of neurons (auto-correlograms) or neuron pairs (crosscorrelograms).

TABLE 2. Numbers and percentages of neurons driven by oscillations of cortical, striatal and SNr LFP

	Cortex $(n = 31)$		Striatum $(n = 20)$		SNr $(n = 36)$	
Entrained by:	(n)	(%)	(n)	(%)	(n)	(%)
Cortex	20	65	12	60	21	58
Striatum	25	81	12	60	28	78
SNr	16	52	11	55	19	53

nothing in the present study indicates that the cortex is the generator of HVSs. Previous experiments have provided strong evidence that thalamocortical reverberating loops are a putative motor for HVS generation (von Krosigk et al., 1993; Tancredi et al., 2000; D'Arcangelo et al., 2002). It has been shown that both normal and pathological HVSs rely on the same fundamental mechanisms, and that thalamocortical network activity may generate the HVSs recorded in healthy rats (Pinault, 2003). The thalamus is also likely to influence the striatum and STN via the intralaminar nuclei (Castle et al., 2005). Of the latter, the parafascicular nucleus is probably involved in spikeand-wave discharges in genetic models of petit mal, as it is involved in seizure regulation (Nail-Boucherie et al., 2005). Consequently, in addition to the cortex, the parafascicular nucleus could provide a second rhythmic input to the striatum during HVSs. Its activity and relationship with the striatum and STN during HVSs in healthy rats, however, still remains to be investigated.

Functional significance of HVSs

The functional significance of HVSs is a matter of debate. It has been proposed that HVSs reflect a state of attentive immobility similar to the µ-rhythm recorded in humans (Nikouline et al., 2000). Although some authors believe that they might allow the enhancement of sensory integration (Nicolelis & Fanselow, 2002), in a recent study they were also associated with withdrawal from an environmental context (Fontanini & Katz, 2005). Another hypothesis is suggested by observing striking similarities with human generalised absence epilepsy: (i) spike-and-wave patterns; (ii) correlation with clonic facial movements (such as whisker twitching); and (iii) their modulation by antiepileptic drugs, all of which are characteristic of absence epilepsy. This has led some investigators to create a widely used rat model of absence seizures (Danober et al., 1998; Coenen & van Luijtelaar, 2003). Furthermore, it is still debated whether HVSs recorded in normal strains correspond to absence seizure, as is believed in genetic models (Polack & Charpier, 2006). As opposed to

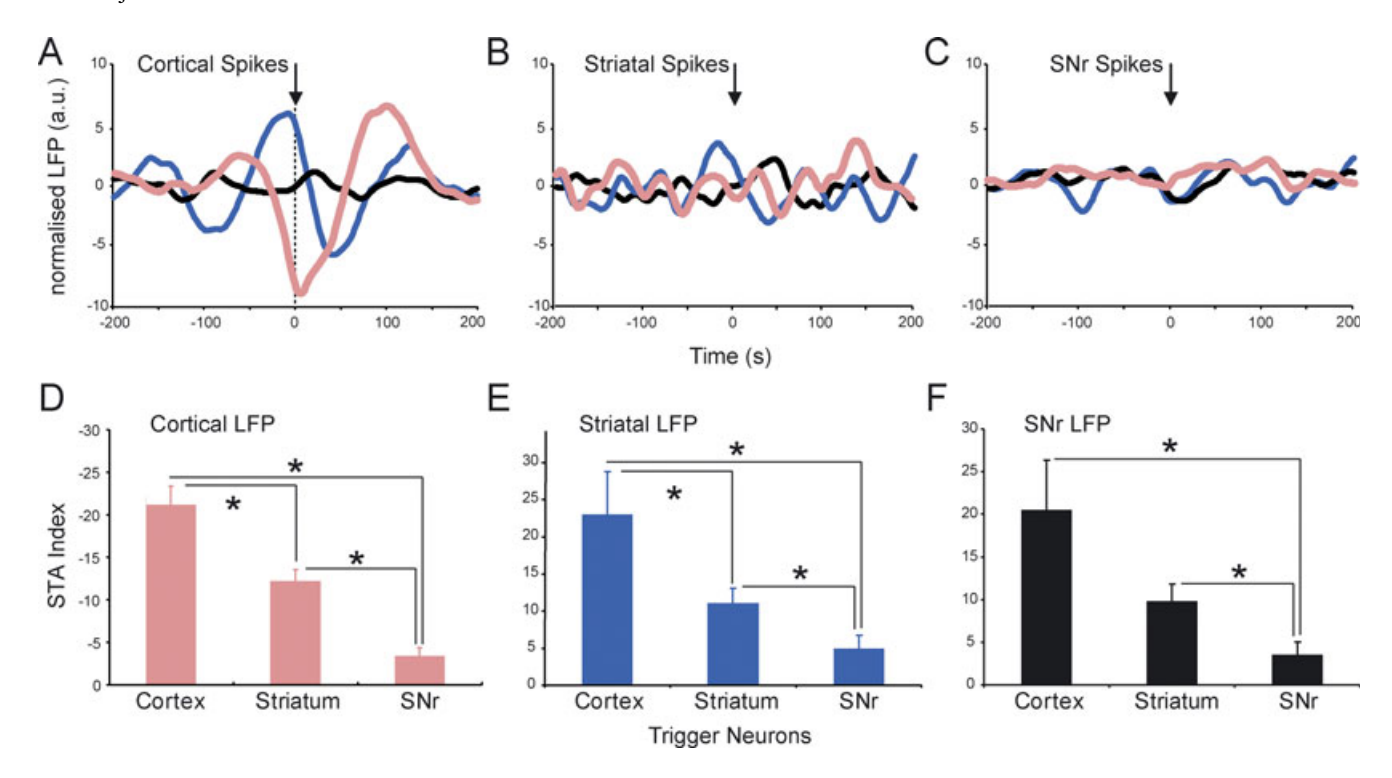


FIG. 6. Spike trigger averaging of LFPs. (A–C) STA of LFPs recorded in the cortex (pink), striatum (blue) and SNr (black) during HVSs. (A) LFPs triggered by motor cortex spikes (n = 20). (B) LFPs triggered by striatum spikes (n = 13). (C) LFPs triggered by SNr spikes (n = 24). LFPs are normalized and expressed in arbitrary units (a.u.; see Materials and methods). (D–F) Comparisons between STA indices for LFPs recorded in motor cortex (pink), striatum (blue) and SNr (black). Each graph shows the STA index for the same structure but with different triggers. Left bar, triggers are cortical spikes; central bar, striatum spikes; right bar, SNr spikes. STA index computation is detailed in Materials and Methods. *P < 0.05 between one index distribution and the next. (D) Index for LFP in the cortex. This index was significantly larger when LFPs were triggered by cortical spikes than by striatum or SNr spikes. (E) Index for LFP in striatum. As described above, this index was significantly larger when LFPs were triggered by cortical spikes rather than by striatum or SNr spikes. (F) Index for LFP in SNr. Here, the indices related to cortex and striatum neurons were not significantly different, although they were significantly larger than that of the SNr neuron.

the results of studies using GAERS rats (Slaght *et al.*, 2004), we did not observe any change in firing frequency between HVSs and other epochs of the recordings. Moreover, behavioural analyses during HVSs revealed that the rats were awake and quietly resting but remained responsive to tactile, auditory and visual stimuli, as shown before (Wiest & Nicolelis, 2003). In contrast, patients suffering from absence epilepsy experience unconsciousness and occasionally move during seizures. In the present study, whisker twitching was not observed during HVSs. Whisker twitching is seen during ictal episodes in genetic rodent models; it is believed to correspond to clonic facial movements related to seizures in patients. Taking these observations into account, it is assumed that the rats observed in the present study did not suffer from absence seizures but exhibited nonpathological HVSs.

The interpretation of the impact of HVSs on the role of BG in movements is rendered difficult by the fact that these spike-and-wave episodes end with the onset of movement (Berke *et al.*, 2004). It is thus difficult to distinguish whether they characterise the absence of action, the onset of a future action or the preclusion of action selection. Motor cortex neurons as well as SNr neurons present strong rhythmic behaviour, and striatal output neurons show clear entrainment into HVSs. However, MSNs do not display a clear oscillatory firing mode despite the robustness of the HVSs recorded in the striatal LFP. This intermittent firing could indicate that the information does not involve the same striatal domains in each oscillation cycle. According to the model proposed by Mink (1996), action selection in the BG is achieved by focusing activity on domains related to specific actions in the BG output structure. Rather than being irregular, the activation of

striatal output neurons would be selective and involved in motor output processing. Nevertheless, the present study did not reveal any clear correlation between HVSs and locomotor activity or whisker twitching, although Nicolelis *et al.* (1995) have shown that HVSs often predict its future occurrence.

Cortex-BG pathways

In the present study, cortex-BG connectivity was studied without any artificial input, whereas conventional studies in anaesthetized animals use electrical stimulation to force neuronal responses. Using this original approach, the data obtained suggest that HVS transmission follows the hierarchical organization of the cortex-BG network, from cortex to SNr via the striatum. Moreover, early coupling between the cortex, striatum and SNr troughs, and late coupling between the cortex and SNr peaks, are likely to represent distinct top-down anatomofunctional channels (Fig. 7). Studies carried out in anaesthetized animals show that frontal or prefrontal cortical stimulations can elicit complex responses in the SNr or the globus pallidus pars interna (Maurice et al., 1999; Nambu et al., 2000; Kolomiets et al., 2003). Authors often report multiple patterns of activation but most notably a triphasic response in the majority of SNr neurons, with an excitationinhibition-excitation temporal organization. Each component of this response has been attributed to the activation of one of the three BG pathways with, in chronological order, the trans-subthalamic hyperdirect pathway (between ~ 7 and ~ 16 ms, excitatory), the transstriatal direct pathway (between ~ 10 and ~ 30 ms, inhibitory), and the indirect pathways (between ~ 25 and ~ 50 ms, excitatory). The

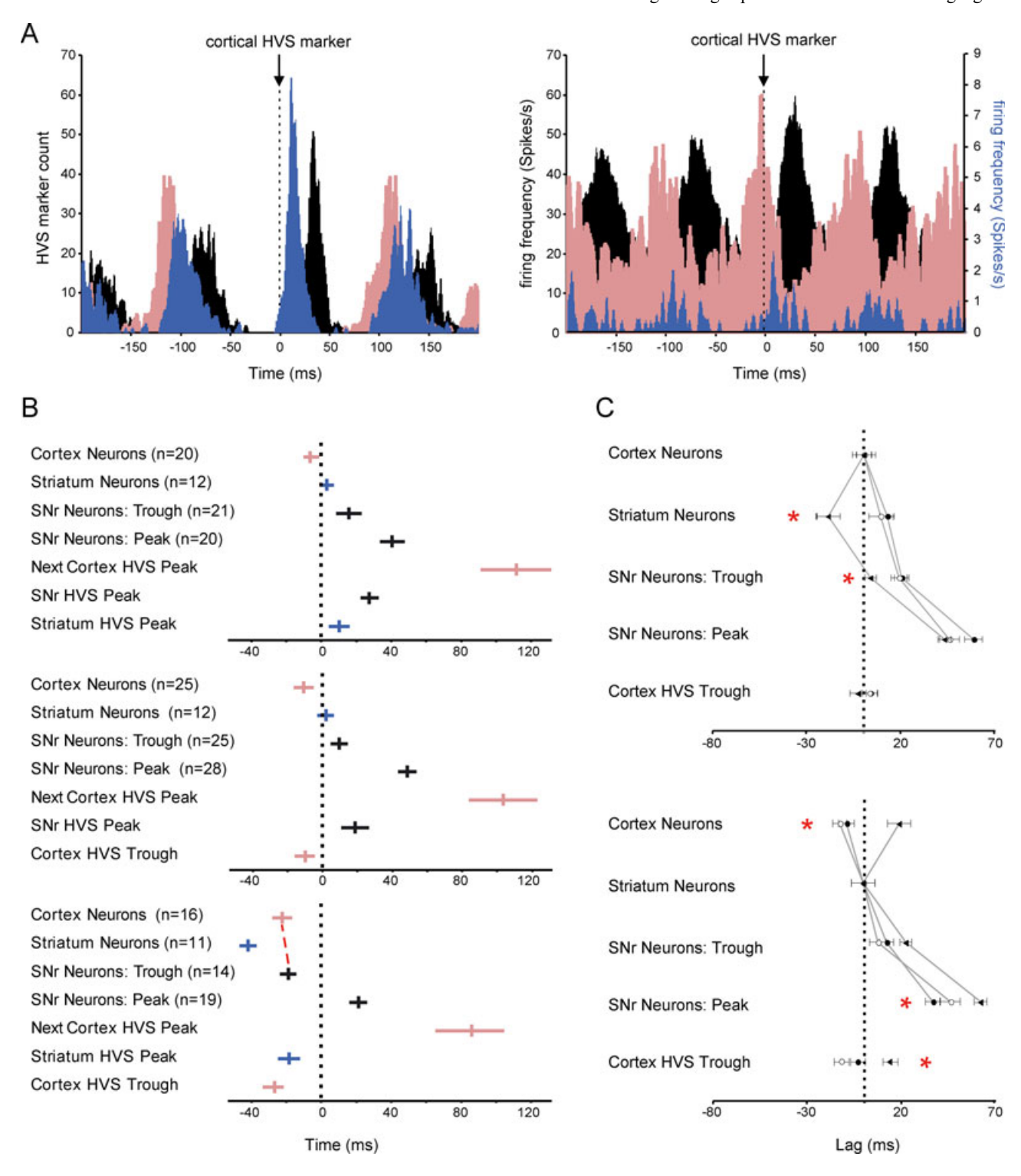


FIG. 7. Neuronal and LFP timing during HVSs. (A) Peri-event histogram triggered on HVS peak markers in the cortex (dotted line). (Left) Peri-event histogram for LFP peak markers. Pink bars, LFP markers in the cortex; blue bars, in striatum; black bars, in SNr. (Right) Peri-event histograms for three neuron spike trains recorded during the same session. Pink bars, neuron in cortex; blue bars, in striatum; black bars, in SNr. The left ordinal scale is for SNr neurons and the right scale is for cortical and striatal neurons. (B) Time-lag distributions showing neuron firing peak times and LFP peak times when triggered by LFP markers in the cortex (top), striatum (middle) and SNr (bottom). For the time plot of each peak or trough, the vertical bar represents the mean value of peak times and the horizontal bar is the SEM. LFP marker distributions were all significantly different. Neuron peak distributions were all significantly different except for those corresponding to the cortex and SNr troughs when triggered by SNr LFP markers, as indicated by the red dotted line (bottom). (C) Single neurons and cortical LFP timings centred on the mean timing of cortical and striatal neurons (bottom). (Top) When triggered by cortical (•) or striatal (○) LFP markers, peak time distributions were similar. However, triggering with SNr LFP markers (◀) induced significant shifts of the striatal peak and SNr trough towards negative time values. LFP markers did not present significantly dissimilar distributions, no matter which trigger was used. (Bottom) Single neurons and cortical LFP timings were centred on the mean timing of striatal neurons. As described above, when triggered by cortical (①) crstriatal (①) LFP markers peak time distributions were not significantly different, whereas triggering with SNr LFP markers () induced significant shifts of the striatal peak and SNr trough. However, cortical LFP markers centred on the cortical neuron peak had significantly dissimilar distributions in the case of SNr triggering. *P < 0.05 between distributions. The error bars represent SEM.

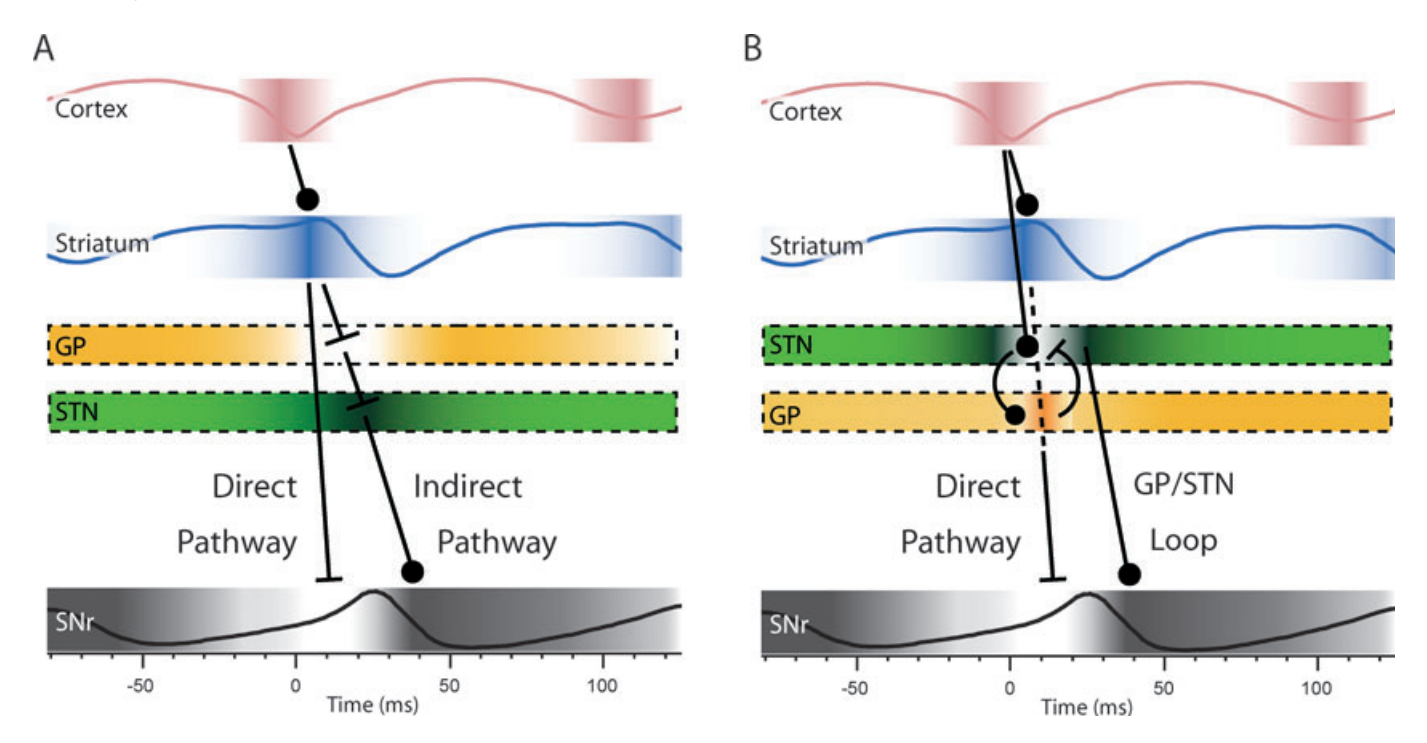


FIG. 8. Two hypotheses for the temporal relationship between the LFP and neuronal activity. (A) According to the classical model of BG, activation of the direct pathway results in early nigral inhibition, and late excitation reflects glutamatergic input from the STN (indirect pathway). (B) Besides activation of the direct and indirect pathways, the GP–STN loop might be involved. Corticosubthalamic inputs could initiate this loop. They could then be amplified through GP–STN reverberating activity and finally be sent to the SNr. Activity of projecting neurons is shown in colour-scaled bands with the neuronal firing rate as a function of colour density (from light to dark for small to large values). The mean shape of the LFP is superimposed onto the corresponding neuronal population. The time origin corresponds to the cortical LFP marker. Direct and indirect pathways between striatum and SNr are shown in black (glutamatergic synapses, solid circles; GABAergic synapses, bars). The dashed frames represent the putative activity of GP and STN neurons during HVSs as no activity was recorded in either of these structures.

SNr trough follows the cortical neuron peak with a lag of 18.9 ms and corresponds to the range of inhibition induced through direct pathway activation. The SNr peak time follows the cortical peak with a lag of 46.3 ms and falls into the range of indirect pathway-induced excitation. Based on these observations, two functional schemes are proposed in the frame of connectivity models of the basal ganglia (Albin et al., 1989; Mink, 1996; Smith et al., 1998; Bevan et al., 2002; Nambu et al., 2002). In the first, early nigral inhibition corresponds to activation of the direct pathway and late nigral excitation corresponds to activation of the indirect pathway (Fig. 8A). Recent work with GAERS rats suggests that there are strong interactions between GP and STN during HVSs under the influence of corticosubthalamic inputs (Paz et al., 2005). A second scenario is thus proposed, in which early nigral inhibition also corresponds to activation of the direct pathway but in which late nigral excitation would reflect the activity of the reverberating GP-STN loop (Fig. 8B). Thanks to this mechanism, the weak striatal input could be amplified before reaching the output stage. This is, moreover, consistent with the stable coupling observed between cortex and SNr peak firing times (Fig. 7C, top).

Interestingly, it was not possible to demonstrate any hyperdirect component in SNr spike trains in the present study, although there is evidence that STN is rhythmically activated during HVSs (Magill et al., 2005; Paz et al., 2005). STN neurons have been shown to exhibit triphasic activation in anaesthetized GAERS rats (Paz et al., 2005), although the early activation which follows the cortical trough attributed to the hyperdirect pathway is weak (< 1 spike per cycle), when compared with the late activation attributed to the indirect pathway (one burst of several spikes). Recent studies show that SNr neurons are more efficiently driven by GABAergic than by

glutamatergic inputs in freely moving rats (Windels & Kiyatkin, 2004). Therefore, it is likely that the influence of the hyperdirect pathway on the SNr is masked by the direct pathway. Subthalamic–nigral transmission during HVSs nevertheless remains to be clarified.

Intrastriatal connections are also likely to play a role during HVSs, through the activity of cholinergic and fast spiking GABAergic interneurons (Tepper et al., 2004). Fast spiking interneurons directly inhibit MSN neurons (Koos & Tepper, 1999; Mallet et al., 2005). Similarly to the latter, the former receive widespread cortical inputs (Ramanathan et al., 2002) and some collaterals from intralaminar thalamic nuclei (Ichinohe et al., 2001). They have also been shown to be driven into spike-and-wave rhythm in normal (Berke et al., 2004) as well as GAERS (Slaght et al., 2004) rats. In both studies, fast spiking interneurons precede the activation of MSN neurons and probably exert an inhibition on MSNs. This GABAergic microcircuit is likely to gate cortical information before it reaches the output stage of the striatum, and thus to play an important role in oscillation propagation through the striatum.

Conclusion

Our study shows that the cortex, striatum and SNr are bound by oscillatory interactions in the freely moving rat, therefore confirming data obtained with individual structure recordings: HVSs propagate from the cortex to SNr via the striatum. This functional connectivity can be observed at the population level (LFP) as well as the single-neuron level. It has also been shown that cortical neurons have the most critical influence on the network. To understand how a signal is computed in the BG during such oscillations, it is necessary to have

close insight into the mechanism by which input nuclei integrate cortical inputs. Dopamine probably orchestrates this information processing because it has been shown to modulate MSN integrative properties (Goto & O'Donnell, 2002; O'Donnell, 2003). Oscillations in the STN and the GP have been found in parkinsonian patients and animal models of this disease (Bergman et al., 1994; Raz et al., 1996; Raz et al., 2000; Raz et al., 2001; Meissner et al., 2006), and are thought to play a role in its physiopathology. Consequently, multipleelectrode recordings of HVS episodes in dopamine-depleted animals could be useful in clarifying the relationship between physiological and pathological oscillations.

Acknowledgements

The authors would like to thank Sandra Dovero and Laura Cardoit for their histology work. This work was supported by the Centre National de la Recherche Scientifique and the Fondation de France. C.D. was funded by the Association France Parkinson and the Boehringer-Ingelheim Fonds.

Abbreviations

BG, basal ganglia; CL, confidence limit(s); GAERS, genetically absence epilepsy rat from Strasbourg; GP, globus pallidus; HVS, high-voltage spindle; LFP, local field potential; MSN, medium spiny neuron; SNr, substantia nigra pars reticulata; STA, spike trigger averaging; STN, subthalamic nucleus.

References

- Albin, R.L., Young, A.B. & Penney, J.B. (1989) The functional anatomy of basal ganglia disorders. Trends Neurosci., 12, 366-375.
- Bartho, P., Hirase, H., Monconduit, L., Zugaro, M., Harris, K.D. & Buzsaki, G. (2004) Characterizationization of neocortical principal cells and interneurons by network interactions and extracellular features. J. Neurophysiol., 92, 600-
- Bergman, H., Wichmann, T., Karmon, B. & DeLong, M.R. (1994) The primate subthalamic nucleus. II. Neuronal activity in the MPTP model of parkinsonism. J. Neurophysiol., 72, 507-520.
- Berke, J.D., Okatan, M., Skurski, J. & Eichenbaum, H.B. (2004) Oscillatory entrainment of striatal neurons in freely moving rats. Neuron, 43, 883-896.
- Bevan, M., Magill, P., Terman, D., Bolam, J. & Wilson, C. (2002) Move to the rhythm: oscillations in the subthalamic nucleus-external globus pallidus network. Trends Neurosci., 25, 525-531.
- Boraud, T., Brown, T., Goldberg, J.A., Graybiel, A.M. & Magill, P.J. (2005) Oscillations in the basal banglia: the good, the bad and the unexpected. In Bolam, J.P., Ingham, C.A. & Magill, P.J. (eds), The Basal Ganglia VIII. Springer, Berlin, pp. 3–24.
- Brown, P. (2003) Oscillatory nature of human basal ganglia activity: Relationship to the pathophysiology of Parkinson's disease. Mov. Disord, 18, 357-363.
- Brown, P., Kupsch, A., Magill, P.J., Sharott, A., Harnack, D. & Meissner, W. (2002) Oscillatory local field potentials recorded from the subthalamic nucleus of the alert rat. Exp. Neurol., 177, 581-585.
- Castle, M., Aymerich, M.S., Sanchez-Escobar, C., Gonzalo, N., Obeso, J.A. & Lanciego, J.L. (2005) Thalamic innervation of the direct and indirect basal ganglia pathways in the rat: Ipsi- and contralateral projections. J. Comp. Neurol., 483, 143-153.
- Coenen, A.M.L. & van Luijtelaar, E.L.J.M. (2003) Genetic animal models for absence epilepsy: a review of the WAG/Rij strain of rats. Behav. Genet., 33,
- D'Arcangelo, G., D'Antuono, M., Biagini, G., Warren, R., Tancredi, V. & Avoli, M. (2002) Thalamocortical oscillations in a genetic model of absence seizures. Eur. J. Neurosci., 16, 2383-2393.
- Danober, L., Deransart, C., Depaulis, A., Vergnes, M. & Marescaux, C. (1998) Pathophysiological mechanisms of genetic absence epilepsy in the rat. *Prog.* Neurobiol., 55, 27-54.
- Deniau, J.M., Menetrey, A. & Charpier, S. (1996) The lamellar organization of the rat substantia nigra pars reticulata: segregated patterns of striatal afferents and relationship to the topography of corticostriatal projections. Neuroscience, 73, 761-781.

- Deransart, C., Hellwig, B., Heupel-Reuter, M., Leger, J.F., Heck, D. & Lucking, C.H. (2003) Single-unit analysis of substantia nigra pars reticulata neurons in freely behaving rats with genetic absence epilepsy. Epilepsia, 44, 1513-1520.
- Fontanini, A. & Katz, D.B. (2005) 7-12 Hz activity in rat gustatory cortex reflects disengagement from a fluid self-administration task. J. Neurophysiol., 93, 2832-2840.
- Goldberg, J.A., Kats, S.S. & Jaeger, D. (2003) Globus pallidus discharge is coincident with striatal activity during global slow wave activity in the rat. J. Neurosci., 23, 10058-10063.
- Goldberg, J.A., Rokni, U., Boraud, T., Vaadia, E. & Bergman, H. (2004) Spike synchronization in the cortex-basal ganglia networks of parkinsonian primates reflects global dynamics of the local field potentials. J. Neurosci., **24**. 6003–6010.
- Goto, Y. & O'Donnell, P. (2002) Timing-dependent limbic-motor synaptic integration in the nucleus accumbens. Proc. Natl Acad. Sci. USA, 99, 13189-13193
- Graybiel, A.M. (1995) Building action repertories: memory and learning functions of the basal ganglia. Curr. Op Neurobiol., 5, 733–741.
- Graybiel, A.M., Aosaki, T., Flaherty, A.W. & Kimura, M. (1994) The basal ganglia and adaptive motor control. Science, 265, 1826-1831.
- Hutchison, W.D., Dostrovsky, J.O., Walters, J.R., Courtemanche, R., Boraud, T., Goldberg, J. & Brown, P. (2004) Neuronal oscillations in the basal ganglia and movement disorders: evidence from whole animal and human recordings. J. Neurosci., 24, 9240-9243.
- Ichinohe, N., Iwatsuki, H. & Shoumura, K. (2001) Intrastriatal targets of projection fibers from the central lateral nucleus of the rat thalamus. Neurosci. Lett., 302, 105-108.
- Kandel, A. & Buzsáki, G. (1997) Cellular-synaptic generation of sleep spindles, spike-and-wave discharges, and evoked thalamocortical responses in the neocortex of the rat. J. Neurosci., 17, 6783-6797.
- Kolomiets, B.P., Deniau, J.M., Glowinski, J. & Thierry, A.M. (2003) Basal ganglia and processing of cortical information: functional interactions between trans-striatal and trans-subthalamic circuits in the substantia nigra pars reticulata. Neuroscience, 117, 931-938.
- Koos, T. & Tepper, J.M. (1999) Inhibitory control of neostriatal projection neurons by GABAergic interneurons. Nat. Neurosci., 2, 467-472.
- von Krosigk, M., Bal, T. & McCormick, D.A. (1993) Cellular mechanisms of a synchronized oscillation in the thalamus. Science, 261, 361-364.
- Magill, P.J., Sharott, A., Harnack, D., Kupsch, A., Meissner, W. & Brown, P. (2005) Coherent spike-wave activity in the cortex and subthalamic nucleus of the freely moving rat. Neuroscience, 132, 659-664.
- Magill, P.J., Sharrot, A., Bevan, M.D., Brown, P. & Bolam, J.P. (2004) Synchronous unit activity and local field potentials in the subthalamic nucleus by cortical stimulation. J. Neurophysiol., 92, 700-714.
- Mailly, P., Charpier, S., Menetrey, A. & Deniau, J.M. (2003) Threedimensional organizationization of the recurrent axon collateral network of the substantia nigra pars reticulata neurons in the rat. J. Neurosci., 23, 5247-5257.
- Mallet, N., Le Moine, C., Charpier, S. & Gonon, F. (2005) Feedforward inhibition of projection neurons by fast-spiking GABA interneurons in the rat striatum in vivo. J. Neurosci., 25, 3857-3869.
- Masimore, B., Schmitzer-Torbert, N.C., Kakalios, J. & Redish, A.D. (2005) Transient striatal gamma local field potentials signal movement initiation in rats. Neuroreport, 16, 2021-2024.
- Maurice, N., Deniau, J.M., Glowinski, J. & Thierry, A.M. (1999) Relationships between the prefrontal cortex and the basal ganglia in the rat: physiology of the cortico-nigral circuits. J. Neurosci., 19, 4674–4681.
- Meissner, W., Ravenscroft, P., Reese, R., Harnack, D., Morgenstern, R., Kupsch, A., Klitgaard, H., Bioulac, B., Gross, C.E., Bezard, E. & Boraud, T. (2006) Increased slow oscillatory activity in substantia nigra pars reticulata triggers abnormal involuntary movements in the 6-OHDA-lesioned rat in the presence of excessive extracellular striatal dopamine. Neurobiol. Dis., 22,
- Mink, J.W. (1996) The basal ganglia: focused selection and inhibition of competing motor programs. Prog. Neurobiol., 50, 381-425.
- Nail-Boucherie, K., Le-Pham, B.-T., Gobaille, S., Maitre, M., Aunis, D. & Depaulis, A. (2005) Evidence for a role of the parafascicular nucleus of the thalamus in the control of epileptic seizures by the superior colliculus. Epilepsia, 46, 141–145.
- Nambu, A., Tokuno, H., Hamada, I., Kita, H., Imanishi, M., Akazawa, T., Ikeuchi, Y. & Hasegawa, N. (2000) Excitatory cortical inputs to pallidal neurons via the subthalamic nucleus in the monkey. J. Neurophysiol., 84, 289-300.

- Nicolelis, M.A., Baccala, L.A., Lin, R.C. & Chapin, J.K. (1995) Sensorimotor encoding by synchronous neural ensemble activity at multiple levels of the somatosensory system. *Science*, 268, 1353–1358.
- Nicolelis, M.A. & Fanselow, E.E. (2002) Thalamocortical [correction of Thalamcortical] optimization of tactile processing according to behavioral state. *Nat. Neurosci.*, 5, 517–523.
- Nikouline, V.V., Wikstrom, H., Linkenkaer-Hansen, K., Kesaniemi, M., Ilmoniemi, R.J. & Huttunen, J. (2000) Somatosensory evoked magnetic fields: relation to pre-stimulus mu rhythm. *Clin. Neurophysiol.*, **111**, 1227–1233
- O'Donnell, P. (2003) Dopamine gating of forebrain neural ensembles. *Eur. J. Neurosci.*, **17**, 429–435.
- Parent, A. & Hazrati, L.-N. (1995) Functional anatomy of the basal ganglia. I. The cortico-basal ganglia-thalamo-cortical loop. *Brain Res. Rev.*, 20, 91–127.
- Paxinos, G. & Watson, C. (1998) The Rat Brain in Stereotaxic Coordinates, 4th edn. Academic Press, New York.
- Paz, J.T., Deniau, J.M. & Charpier, S. (2005) Rhythmic bursting in the corticosubthalamo-pallidal network during spontaneous genetically determined spike and wave discharges. *J. Neurosci.*, 25, 2092–2101.
- Pinault, D. (2003) Cellular interactions in the rat somatosensory thalamocortical system during normal and epileptic 5–9 Hz oscillations. *J. Physiol.* (Lond.), **552**, 881–905.
- Polack, P.O. & Charpier, S. (2006) Intracellular activity of cortical and thalamic neurones during high-voltage rhythmic spike discharge in Long–Evans rats in vivo. J. Physiol. (Lond.), 571, 461–476.
- Ramanathan, S., Hanley, J.J., Deniau, J.M. & Bolam, J.P. (2002) Synaptic convergence of motor and somatosensory cortical afferents onto GABAergic interneurons in the rat striatum. *J. Neurosci.*, 22, 8158–8169.
- Raz, A., Feingold, A., Zelanskaya, V., Vaadia, E. & Bergman, H. (1996) Neuronal synchronization of tonically active neurons in the striatum of normal and parkinsonian primates. J. Neurophysiol., 76, 2083–2088.
- Raz, A., Frechter-Mazar, V., Feingold, A., Abeles, M., Vaadia, E. & Bergman, H. (2001) Activity of pallidal and striatal tonically active neurons is correlated in MPTP-treated monkeys but not in normal monkeys. J. Neurosci., 21, RC128 (121–125).
- Raz, A., Vaadia, E. & Bergman, H. (2000) Firing patterns and correlations of spontaneous discharge of pallidal neurons in the normal and the tremulous

- 1-methyl-4-phenyl-1,2,3,6-tetrahydropyridine vervet model of parkinsonism. *J. Neurosci.*, **20**, 8559–8571.
- Robinson, D.L., Goldberg, M.E. & Stanton, G.B. (1978) Parietal association cortex in the primate: sensory mechanisms and behavioural modulations. *J. Neurophysiol.*, **41**, 910–932.
- Sharott, A., Magill, P.J., Harnack, D., Kupsch, A., Meissner, W. & Brown, P. (2005) Dopamine depletion increases the power and coherence of beta-oscillations in the cerebral cortex and subthalamic nucleus of the awake rat. *Eur. J. Neurosci.*, 21, 1413–1422.
- Shaw, F.Z. (2004) Is spontaneous high-voltage rhythmic spike discharge in Long Evans rats an absence-like seizure activity? *J. Neurophysiol.*, **91**, 63–77
- Slaght, S.J., Paz, T., Chavez, M., Deniau, J.M., Mahon, S. & Charpier, S. (2004) On the activity of the corticostriatal networks during spike-and-wave discharges in a genetic model of absence epilepsy. J. Neurosci., 24, 6816– 6825
- Smith, Y., Bevan, M.D., Shink, E. & Bolam, J.P. (1998) Microcircuitry of the direct and indirect pathways of the basal ganglia. *Neuroscience*, 86, 353– 387
- Tancredi, V., Biagini, G., D'Antuono, M., Louvel, J., Pumain, R. & Avoli, M. (2000) Spindle-like thalamocortical synchronization in a rat brain slice preparation. J. Neurophysiol., 84, 1093–1097.
- Tepper, J.M., Koos, T. & Wilson, C.J. (2004) GABAergic microcircuits in the neostriatum. *Trends Neurosci.*, 27, 662–669.
- Tseng, K.Y., Kasanetz, F., Kargieman, L., Riquelme, L.A. & Murer, M.G. (2001) Cortical slow oscillatory activity is reflected in the membrane potential and spike trains of striatal neurons in rats with chronic nigrostriatal lesions. *J. Neurosci.*, 21, 6430–6439.
- Vergnes, M., Marescaux, C. & Depaulis, A. (1990) Mapping of spontaneous spike and wave discharges in Wistar rats with genetic generalized nonconvulsive epilepsy. *Brain Res.*, 523, 87–91.
- Wiest, M.C. & Nicolelis, M.A. (2003) Behavioral detection of tactile stimuli during 7–12 Hz cortical oscillations in awake rats. *Nat. Neurosci.*, 6, 913– 914
- Windels, F. & Kiyatkin, E.A. (2004) GABA, not glutamate, controls the activity of substantia nigra reticulata neurons in awake, unrestrained rats. J. Neurosci., 24, 6751–6754.
- Windels, F. & Kiyatkin, E.A. (2006) General anesthesia as a factor affecting impulse activity and neuronal responses to putative neurotransmitters. *Brain Res.*, 1086, 104–116.